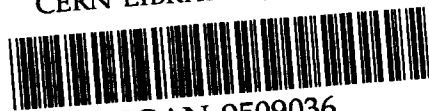


DD

E7-95-148

CERN LIBRARIES, GENEVA



SCAN-9509036


su 9536

THE FOBOS* 4π -DETECTOR
OF CHARGED PARTICLES AT THE FLNR
OF THE JINR DUBNA

FOBOS Collaboration

*The FOBOS project is financially supported by the BM-BWFT,
Germany, under the contract No.: 06 DR 671


1995



Макет Т.Е.Попеко

Подписано в печать 5.04.95
Формат 60×90/16. Офсетная печать. Уч.-изд.листов 3,01
Тираж 400. Заказ 48114. Цена 1806 р.

Издательский отдел Объединенного института ядерных исследований
Дубна Московской области



1. BASIC PRINCIPLES OF FOBOS

The main task of FOBOS is to identify the charged products from heavy-ion induced reactions in the medium energy region of $10 + 100$ AMeV.

A multi-detector principle was chosen using such type of cells which can handle only one particle of a certain multiple event. As it is impossible to cover by only one detector-shell the whole energy dynamic range expected for all sorts of particles which can be emitted, different types of particle detectors had to be combined in one detector module. Altogether 30 modules are arranged at a monolithic central vacuum chamber looking from the outside like a truncated icosahedron (20 regular hexagons and 10 regular pentagons). This geometrical decision was governed by the parameters of the U - 400 M, the basic heavy-ion accelerator for FOBOS. As the required energies are reached at this machine for light- and medium-mass ions only, experiments should be performed in direct kinematics. Consequently, considering the possible momentum transfer, the velocity of the compound system stays relatively moderate, and most of the fragments can be emitted into all directions of the laboratory system.

The granularities chosen are related to the multiplicities expected for different types of particles : The 30 position-sensitive avalanche counters (PSAC) of the first detector-shell and the 30 axial (Bragg) ionization chambers (BIC) of the second one are able to register and to identify 2 ... 5 heavy and intermediate-mass fragments. More penetrating fragments and light charged particles (LCP) produced with a higher multiplicity are detected in a third scintillator shell consisting of 210 CsI(Tl) counters. An array of 96 phoswich detectors can be placed into the forward cone to record fast early-phase particles.

The geometrical coverage of the first shell amounts to 60% of 4π . Mechanical constraints as well as other considerations (technology, price etc.) slightly lower the efficiency of the further detector shells.

A scheme of FOBOS is shown in fig. 1. The detector signals measured and the physical quantities derived from them are illustrated in fig 2. The flight-path from the target to the PSAC amounts to 50 cm what enables an accurate measurement of the fragment velocity vectors. The depth of the BIC is 25 cm. Depending on the polar angle θ , thicknesses of the CsI(Tl)-crystals of $10 + 15$ mm are used. The phoswich detectors of the forward array consist of a 0.5 mm thick layer of fast-plastic scintillator combined with 20 mm of BGO. The energy dynamic range of the FOBOS detector is drawn in fig. 3.

2. THE POSITION-SENSITIVE AVALANCHE COUNTERS

Presently, PSAC are well established charged particle detectors. The large-area PSAC of FOBOS are able to register fragments ranging from low-energy alpha particles up to fission fragments (FF) and heavy evaporation-residue nuclei (ER) (fig3). To lower the registration threshold, very thin foils ($1.2 \mu\text{m}$ polyester) had to

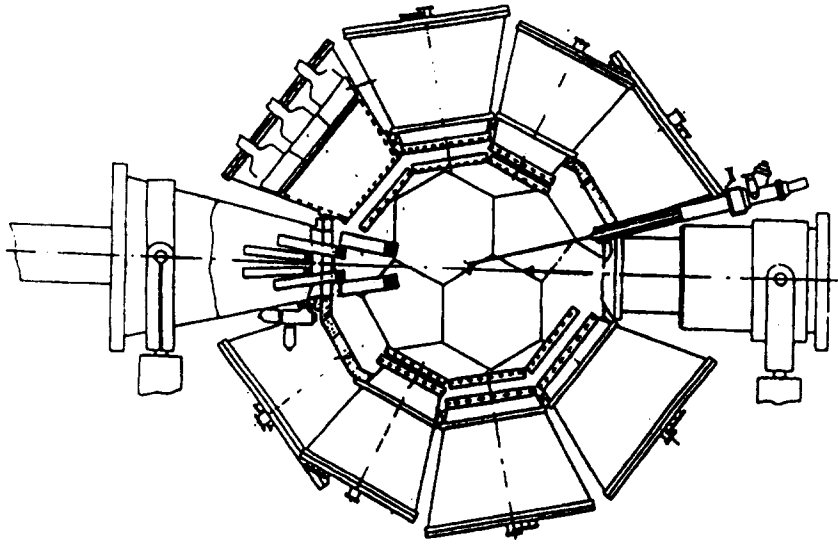


Fig. 1 Schematical view of the FOBOS detector.

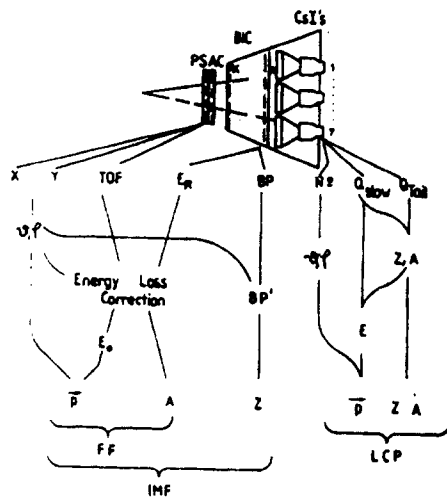


Fig. 2 Measured and derived quantities at the FOBOS detector.

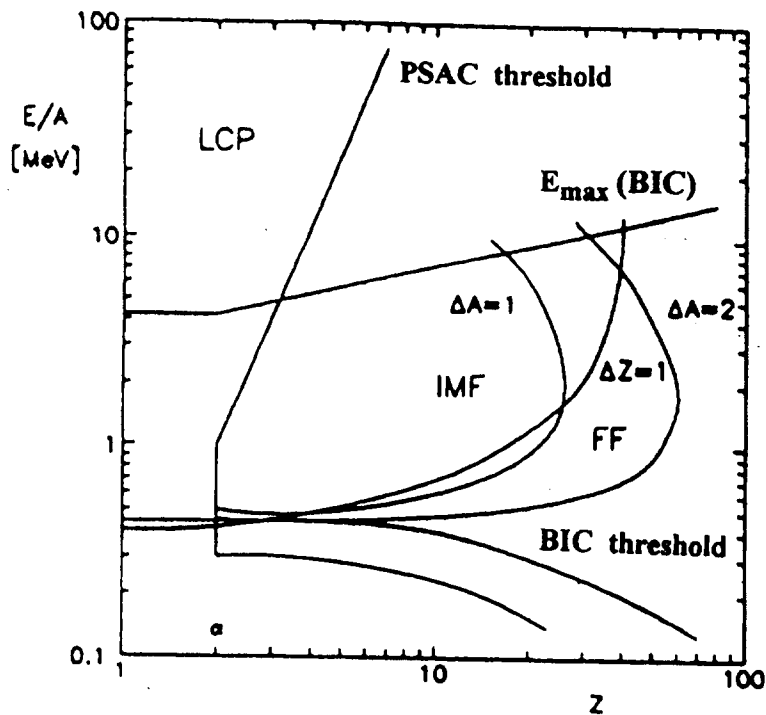


Fig. 3 Estimated dynamic ranges of the gas-detectors of FOBOS in dependence of Z and E/A of the measured particles. For explanation of the symbols see text.

be utilized for the entrance- and exit-windows and the central gilded cathode. Two anode wire planes (30 μm thick Cu-Be wires spaced by 1.0 mm) serve as coordinate grids. A mechanical precision of 50 μm is required for the 3 mm spaced sensitive gaps. The counter frames have pentagonal or hexagonal shapes leaving circular sensitive areas of diameters 243 mm and 327 mm, respectively.

The PSAC are mounted to the front-side of the BIC and usually operated with pentane gas in a flow-through regime at pressures of 200 + 800 Pa.

The read-out principle of the PSAC is illustrated in fig. 4. The negative detector bias is fed to the cathode. The cathode read-out circuit delivers an 80-fold amplified current signal for timing and a charge signal of 150 mV/pC sensitivity for pulse-height analysis. The amplifier is isolated from the high voltage (bias 1.5 kV, filter time 0.5 s). The timing signal may be directly fed into the trigger circuit.

Every two neighboring anode wires are connected with a conductive strip capacitively coupled to a wound delay-line. The two lines have 1.4 ns/mm specific delay and 50 Ω impedance. They are matched with resistors at one end and

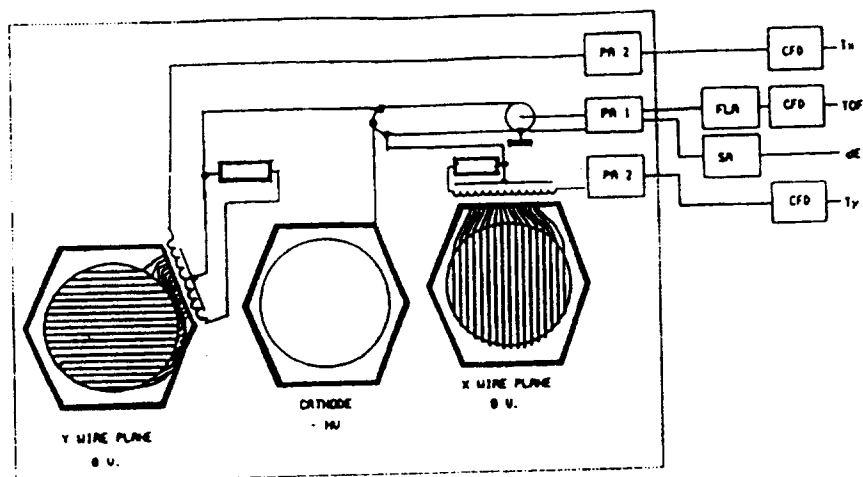


Fig. 4 Read-out principle of the position-sensitive avalanche counter.

coupled to read-out amplifiers with 560Ω "cold" dynamical input resistance and 800-fold current amplification at the other end.

All channels are protected against damage for the case of spark discharges in the gas. The laboratory-made SMD circuits are placed directly on the counter frames.

The three constant-fraction discriminators (CFD) are housed in a single CAMAC module. Their thresholds are CAMAC-controlled. The wide dynamic range (1000:1) allows to cover all experimental conditions without changing the amplification factor of the preamplifiers. The time walk is ± 50 ps for step pulses of 2 ns risetime in the range of $10 \text{ mV} + 2\text{V}$.

The intrinsic timing resolution of the PSAC amounts to ≈ 200 ps. It is position-dependent and corrected off-line. Fig. 5 shows a time spectrum of a ^{226}Ra alpha-particle source measured against a small Start-counter, fig. 6 a coordinate spectrum.

Counts TOF-spectra Ra-226 Counter 126

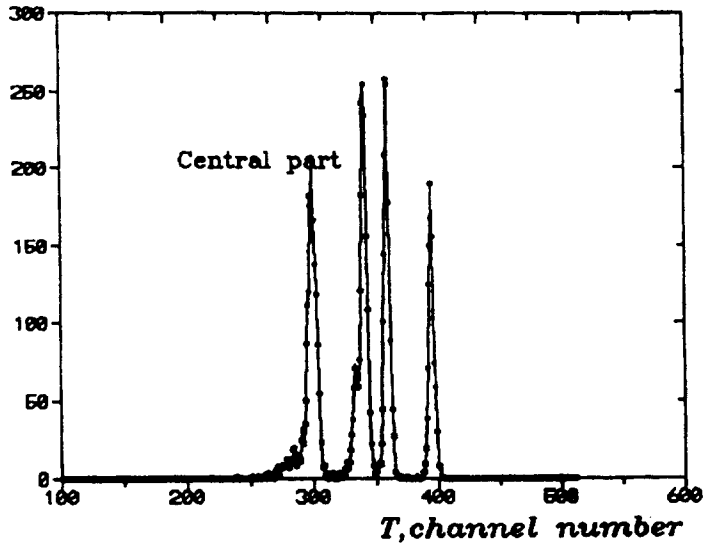


Fig. 5 Time spectrum of a PSAC (central part).

counts X-spectra Ra-226 Counter 117

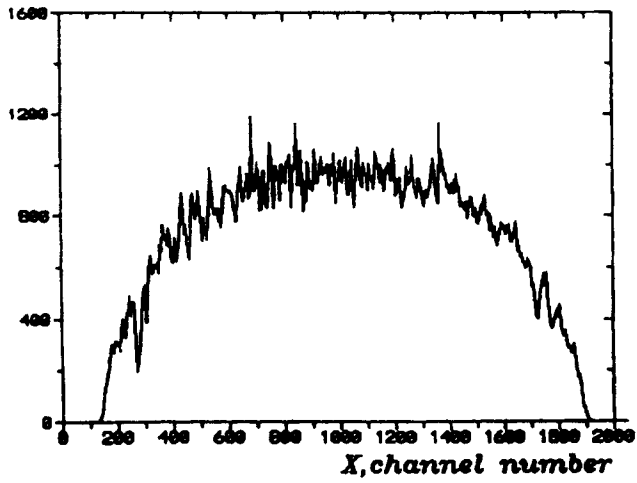


Fig. 6 Coordinate spectrum of a PSAC.

3. THE AXIAL IONIZATION CHAMBERS

The Bragg-curve ionization chambers cover cones of $\pm 13.8^\circ$ and $\pm 17.4^\circ$ with entrance-window diameters of 285 mm and 385 mm, respectively. The thin entrance-window foils (cathodes: $1.5 \div 3 \mu\text{m}$ thick aluminized polyester) must be supported by a twofold structure - a main carrier with a transparency of 94 % and an etched Ni-mesh (cell $\varnothing 2.7 \text{ mm}$) with a transparency of 66 %. Up to now, the last number causes the most serious restriction to the solid angle. However, cells smaller in diameter than $\varnothing 3 \text{ mm}$ are necessary because, otherwise, the foils would not hold a gas pressure of 100 kPa needed to stop most of the intermediate-mass fragments within the BIC-depth of 25 cm.

The axial-field shaping is performed by 5 mm spaced Cu-strips coated on the Teflon insulator cone. The voltage-devider soldered to the strips provides equal potential steps, i.e., a homogeneous electric field.

The Frisch-grid consists of two perpendicular planes of $50 \mu\text{m}$ thick and 1 mm spaced Cu-Be wires. The anode placed 10 mm behind the Frisch-grid is made of a $10 \mu\text{m}$ thick aluminized polyester foil. At a gas pressure of 100 kPa an anode potential of + 8 kV is necessary.

The electron drift-time of up to $4 \mu\text{s}$ would cause a large ballistic deficit in the case of conventional pulse-shaping. Therefore a digital processing method has been utilized which derives the energy and Bragg-peak height from digitized signal samples. The principle is illustrated in fig. 7.

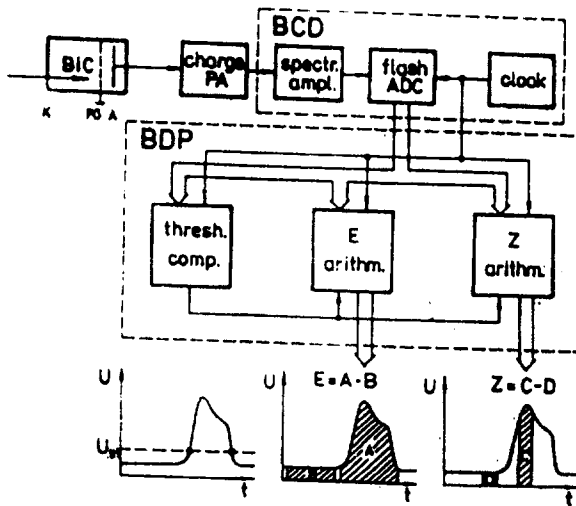


Fig. 7 Principle of the new signal-processing method for Bragg-peak spectroscopy.

The read-out system of the BIC consists of a charge-sensitive preamplifier and two CAMAC modules - the Bragg-curve-digitizer (BCD) and the Bragg-digital-processor (BDP). The Bragg-curve signal is shaped by a spectroscopy amplifier with a short time-constant (0.2 - 0.4 μ s) and digitized by an 8-bit flash ADC with a quartz-stabilized sampling frequency of 10 MHz.

When a signal is recognized by the threshold-comparator, two arithmetic units calculating the energy (E) and the Bragg-peak-height (Z) are activated. The algorithms are schematically displayed at the bottom of fig. 7. The shadowed areas indicate sums of digitized values.

The digital comparator determines the registration threshold, and a pile-up inspector rejects erroneous results. The control of the working conditions and the data transfer is performed via the CAMAC dataway.

The control logics (not shown in fig. 7) realizes the coincidence conditions with the PSAC, the pile-up inspection and the connection with the first-level trigger logics. The digital processing system is faster by a factor of 10 and about two times cheaper than a conventional one and very simple to operate.

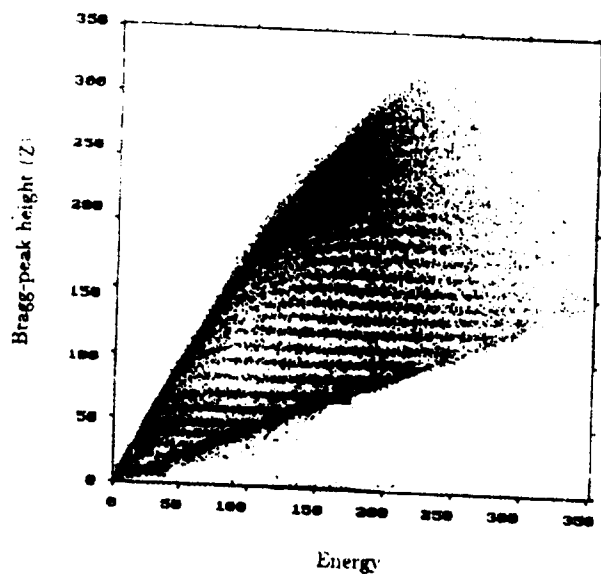


Fig. 8 Bragg-peak-height over energy scatterplot of a BIC.

Fig. 8 shows a Bragg-peak-height over energy scatterplot of fragments measured by a BIC positioned at $\theta = 37.4^\circ$ using the reaction ^{14}N (34 AMeV) + ^{197}Au . Branches for $Z=2+25$ are resolved. The smooth transition to unresolved charge numbers corresponds with the region of light fission fragments.

4. THE SCINTILLATOR SHELL

The scintillator shell consists of mosaics of 7 hexagonal-shaped CsI(Tl)-crystals each, arranged, together with the light guides (LG), magnetic shields and the photomultipliers (PM), behind the anode-foils inside the BIC gas volumes. They cover the BIC cones to about 75 %. This geometry was found to be a compromise between technological and technical requirements, efficiency and price.

The crystal thicknesses of 15 mm (at $\theta \approx 19^\circ \pm 52^\circ$) and 10 mm (at $\theta \approx 53^\circ \pm 162^\circ$) correspond to the ranges for protons (alpha particles) at energies of 64 AMeV and 50 AMeV, respectively.

The signals of the PM are split, delayed and directly fed into 4 charge-integrating 96-channel FASTBUS ADCs to perform pulse-shape analysis for particle discrimination. The gate logics is started by a coincidence between some scintillator event with a permitting event from the gas-detector array. The integration intervals for optimal LCP discrimination are found to be $\Delta t_1 = 0 \pm 400$ ns and $\Delta t_2 = 1600 \pm 3600$ ns. LCP are well separated up to $Z = 3$ (fig. 9).

Every 16 channels are summed to trigger a discriminator which delivers the respective timing signal for a 12-channel TDC to select the true beam bunch. Furthermore, light fragments penetrating the BIC can be analyzed by application of the $\Delta E - E_p$ method to the energy loss (ΔE) in the BIC and the light-output (residual energy E_p) of the scintillators (fig. 10). This considerably enlarges the energy dynamic range of the FOBOS detector and permits energy calibration of the nonlinear CsI(Tl) response.

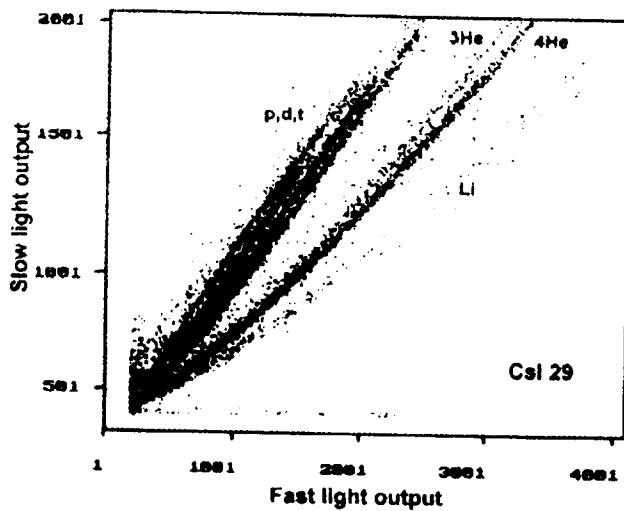


Fig. 9 Pulse-shape discrimination matrix of a CsI(Tl) detector for $^{14}\text{N} + ^{197}\text{Au}$.

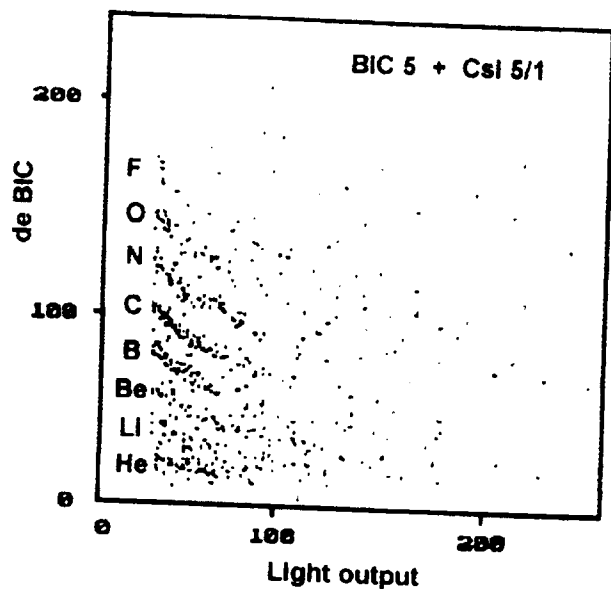


Fig. 10 Particle identification matrix for light fragments.

5. THE FORWARD ARRAY

For a geometrical reason the minimum acceptance angle of the FOBOS spectrometer is $\vartheta \approx 21^\circ$. Mainly forward directed reaction products are ineffectively or not at all registered. On the other hand these particles carry valuable information about the transferred linear momentum in the nuclear reaction, the reaction plane, the excitation energy of the intermediate system, the recoil velocity, etc. Therefore, it has been proposed to modify a part of the former ARGUS detector of the HMI Berlin to be used as a forward array at FOBOS. Six rings of altogether 92 phoswich detectors consisting of 0.5 mm Pilot-U fast scintillator and 20 mm BGO are prepared to be installed into the forward cone of FOBOS. Special mechanics for adaptation has been designed.

Table 1: Geometry of the forward array

Ring	Detectors	ϑ
1	12	5°
2	16	8°
3	16	10.5°
4	16	14°
5	16	18.5°
6	16	23.5°

The geometrical conditions are given in tab. 1. The thickness of the scintillators allows one to stop protons (alpha particles) with energies up to ≈ 100 AMeV. Particle charge identification is possible up to $Z \approx 15$. To include the forward array into the FASTBUS data acquisition system of the scintillator shell a simple pulse-processing concept has been modified for application to phoswich detectors. A special analogue electronics circuit separates the fast light-component from the phoswich signal. This allows to use only one common gate for pulse integration (fig. 11).

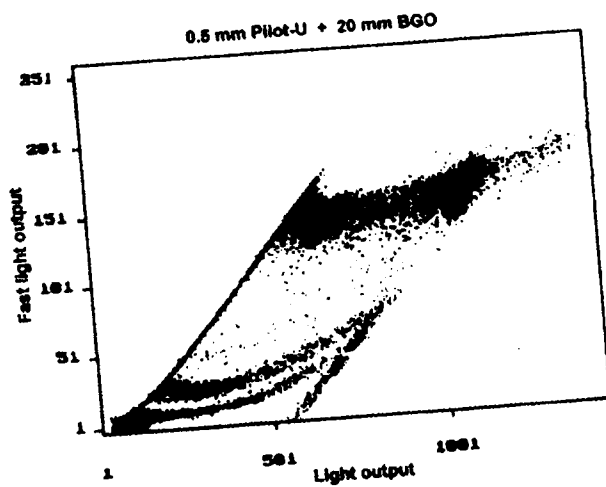


Fig. 11 Scatterplot of a phoswich detector. LCP branches and the scattered ^{14}N beam particles are seen.

6. THE GAS-VACUUM SYSTEM

An automated complex vacuum and gas-supply system has been developed, installed and successfully tested during several FOBOS measurement periods. It controls the secure evacuation (flooding) of the central chamber and the gas-detectors guaranteeing defined pressure gradients to avoid damage of the thin window foils of the PSAC and BIC. Furthermore, it controls the gas flow-through regimes. Providing a full gas exchange inside the gas detector volumes within several hours a pressure stabilization accuracy of better than 1% has been achieved.

A crucial problem of the FOBOS facility is the leakage rate Q through the thin entrance window foils of a great number of gas detectors. Some compromise had to be found between foil thickness and quality, sensible effective pumping speed S_{eff} and reachable ultimate pressure p_{E} inside the central chamber of FOBOS. The measurement of the gas diffusion rate of 1.5 μm thick DuPont Mylar foils gave fo

unsupported test foils (area $A = 13 \text{ cm}^2$) at a difference pressure of 2.67 mbar a value of $Q/A = 3.7 \cdot 10^{-8} \text{ mbar l/s cm}^2$. Extrapolating to a working gas pressure of 267 mbar, a leakage rate of $Q = 4.2 \cdot 10^{-3} \text{ mbar l/s}$ for a BIC with an active window area of $A = 1104 \text{ cm}^2$ and a value of $Q = 2.2 \cdot 10^{-3} \text{ mbar l/s}$ for a BIC with $A = 594 \text{ cm}^2$ are expected. Summing over all 30 BIC modules at 267 mbar yields a total value of $Q = 0.1 \text{ mbar l/s}$ for the theoretical leakage rate of the whole FOBOS facility. The contributions of the PSAC foils are negligible because of a much lower working pressure within the PSAC.

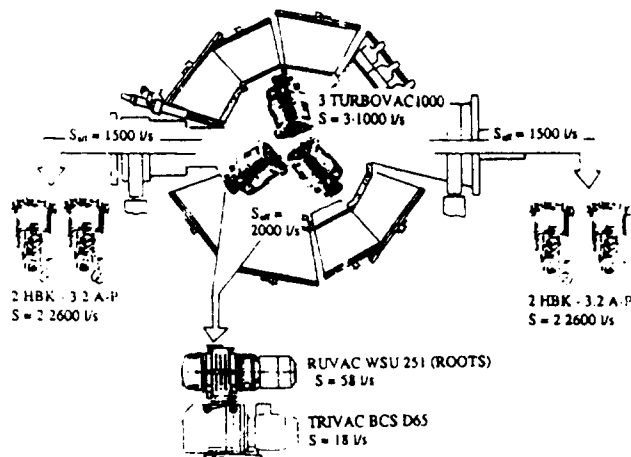


Fig. 12 The FOBOS evacuation system

Tab. 2 shows that the real leakage rates measured during the FOBOS experiments in 1993/1994 were much higher than the expected value of Q .

Tab. 2 : Vacuum values within the central chamber during different experiments.

Exp.	foils [μm]	BIC	$p(P10)$ [mbar]	pumps used	S_{err} [l/s]	Q [mbar l/s]	p_E [mbar]
9/93	1.2	6	117	4 O1 AB - 1500	1500	0.2	$1.3 \cdot 10^{-4}$
10/93	1.2	12	267	3 O1 AB - 1500	1100	0.7	$1.6 \cdot 10^{-3}$
12/93	1.2	12	267	3 O1 AB - 1500 3 Turbovac 1000	3100	6.7	$2.1 \cdot 10^{-3}$
6/94	1.5	8	267	3 Turbovac 1000 4 HBK - 3.2 A-P	5000	0.3	$6.0 \cdot 10^{-5}$
9/94	1.5	16	333	3 Turbovac 1000 3 HBK - 3.2 A-P	4250	0.9	$2.1 \cdot 10^{-4}$

At nearly 2.7 mbar l/s (per pump) the overload threshold for automatic switch-off of a turbomolecular pump OI AB - 1500 is reached. In order to avoid this risk and to increase the total pumping speed these turbomolecular pumps situated at the beam entrance and exit of FOBOS were replaced by cryopumps HBK - 3.2 A-P (S = 2600 l/s). In connection with the LEYBOLD TURBOVAC 1000 (S = 1000 l/s) set-up directly mounted to the central chamber of FOBOS this resulted in an effective pumping speed of altogether 5000 l/s. This pump combination was carefully tested under different load conditions using calibrated leakage rates, generated by special mounted gas-flow controllers. Now long-time leakage rates of even 13.3 mbar l/s can be managed supporting under this condition an ultimate vacuum of $p_E = 3 \cdot 10^{-3}$ mbar.

The pentane gas-supply system for the PSAC is shown in fig. 13. Its status is checked by a SIMICRO-SX microcomputer system and visualized at a X-terminal. The vapor of pentane originating within the glass balloons at room temperature flows through the regulating valve V 11.9 which adjusts the gas flow Q. The second-regulator V 11.0 allows to stabilize the pressure in a range of 1 + 6 mbar inside the gas collector rings of FOBOS to which up to 30 PSAC can be connected. Special sensors (SS) in combination with minivalves (MV) protect the PSAC against critical pressure to avoid a rupture of the thin window foils. The MV is normally closed and opens if p inside the PSAC exceeds a value of about 6.6 mbar. In the first experiments, up to 16 PSAC have been supplied simultaneously. A special technique has been applied to determine the leakage rate Q of each PSAC before mounting it to FOBOS. Therefore, Q of the whole PSAC configuration could be limited to a reasonable value, which is only about one order of magnitude higher than the leakage rate of the central vacuum chamber.

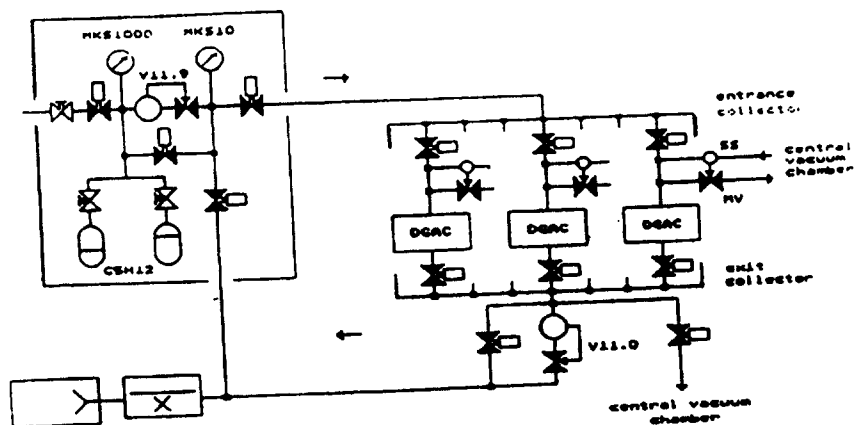


Fig. 13 Scheme of the pentane gas-supply system for the PSAC.

For the preparation of the P10 gas mixture (90% Ar + 10% CH₄) of the BIC an on-line mixing method is applied. This has been found to be necessary to guarantee a good long-time stability of the gas mixture composition and, therefore, of the electron drift-time in the BIC. The gas is mixed by automatic control of two independent electronic mass-flow controllers for the gas components (fig 14). An on-line check of the gas mixture can be performed by means of a LEYBOLD Transceptor gas analyzer.

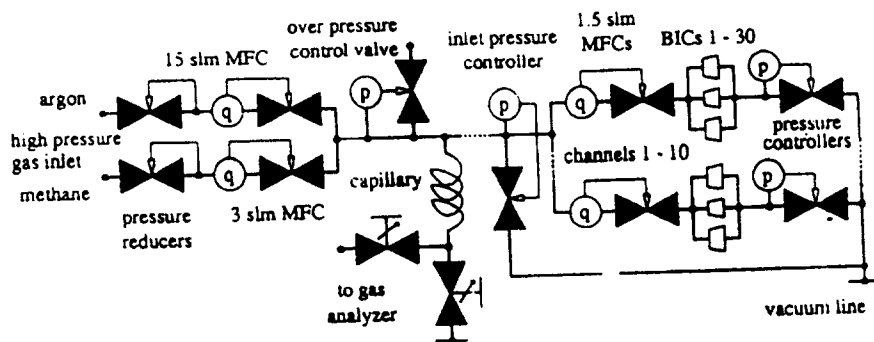


Fig. 14 Scheme of the BIC on-line gas mixing and control system.

The automated evacuation and gas supply system of FOBOS is based on a SIEMENS-SX-Multibus II system and a SUN Sparcstation SLC computer. It controls 64 ADC and 16 DAC channels and 352 digital input and 288 output channels within a Multibus I crate. The necessary cyclic data transfer to the SUN station is realized via special TCP / IP socket programming. Graphical visualization of the system status is realized on an X - terminal (fig. 15).

Furthermore, the state of the whole system is recorded continuously. The pressure-time behavior of any of the 64 measuring points can be displayed on the screen of the SUNstation. Each on-line diagram shows the pressure trend at one of a measuring points during the past 30 minutes. Programs for error handling have been implemented. In case of an error a message window with explaining text is opened and an acoustic signal is warning the user. If some pressure exceeds its permitted range the counter high voltage is switched off automatically.

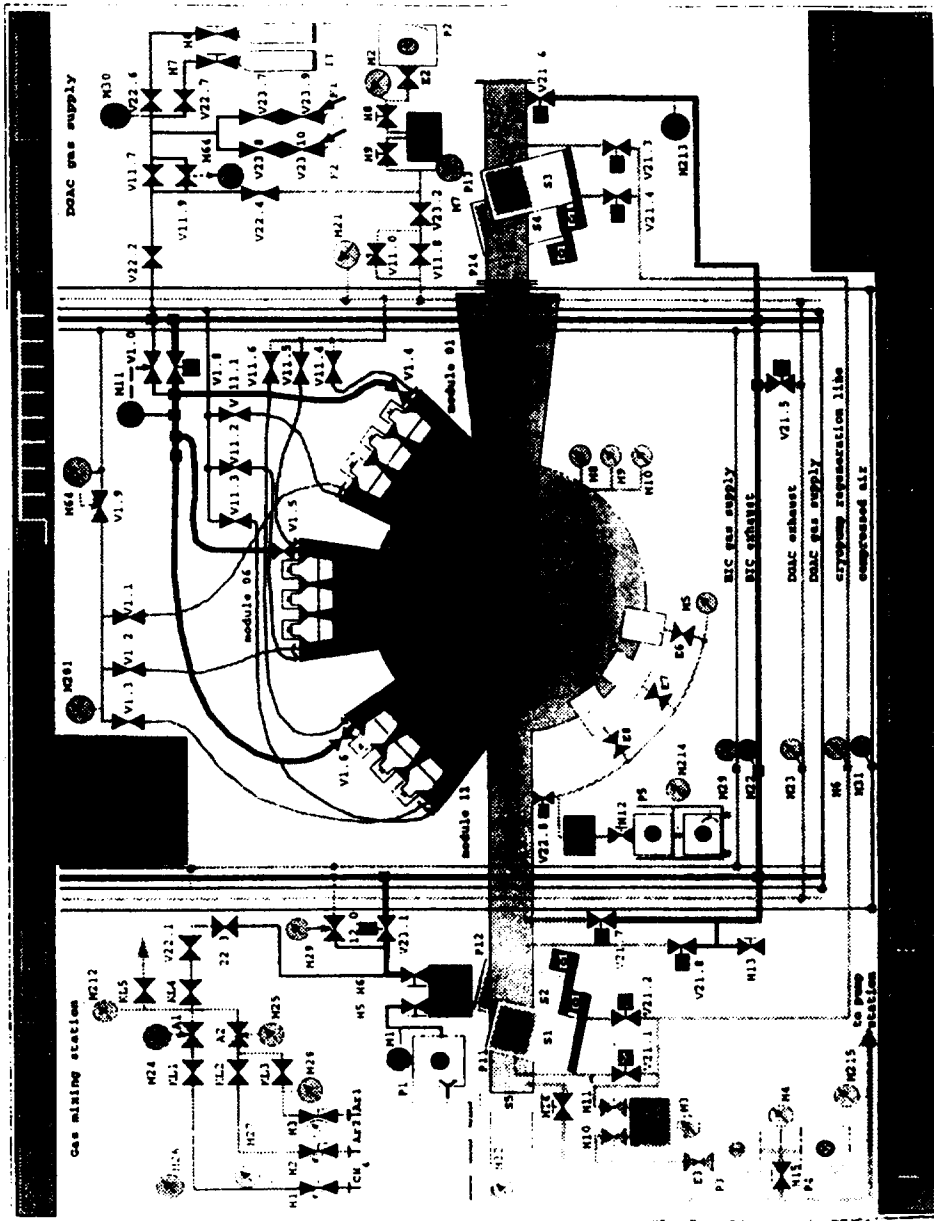


Fig. 15 X - terminal hardcopy of the gas-vacuum system status visualization.

7. THE DATA ACQUISITION SYSTEM

The FOBOS data acquisition system is based on CAMAC-, VME- and FASTBUS hardware and a multiprocessor network connecting 2 SUNstations, a μ VAX, an ELTEC workstation, 2 X-terminals and 4 PC's.

11 CAMAC crates for digitizing and control are connected with the main VME crate by means of the parallel VSB Differential Bus Extension (VDB bus). The VDB bus is well suited for multi-crate systems where different bus standards have to be controlled.

In the main VME crate a single-board computer EUROCOM-6 with 68030 CPU builds the separate data to the event data block. The STR 723 VSB / VDB converter is placed in the ELTEC VME crate at the rear side. It connects the VME Subsystem bus (VSB) to the VDB bus. The STR 723 works in the VSB-Master / VDB-Slave mode.

The CAMAC-to-VSB interface is a single width CAMAC crate controller STR 610 / CBV driven from the VSB via the VSB Differential Cable. The specification of the STR 610 / CBV is similar to the A1-type CAMAC crate controller. The CBV occupies the CAMAC station N=24 and requires a connection to station N=25 via an other CAMAC module, e.g. STR 611 / DMS (CAMAC Dataway-Display and Dummy crate controller). The STR 610 / CBV maps a portion of the VSB address space to the CAMAC "C.N.A.F" and generates single CAMAC cycles from each proper VSB cycle.

Four charge-integrating FASTBUS ADC's (C.A.E.N. F683C) are used for the photomultiplier read-out of the scintillator shell

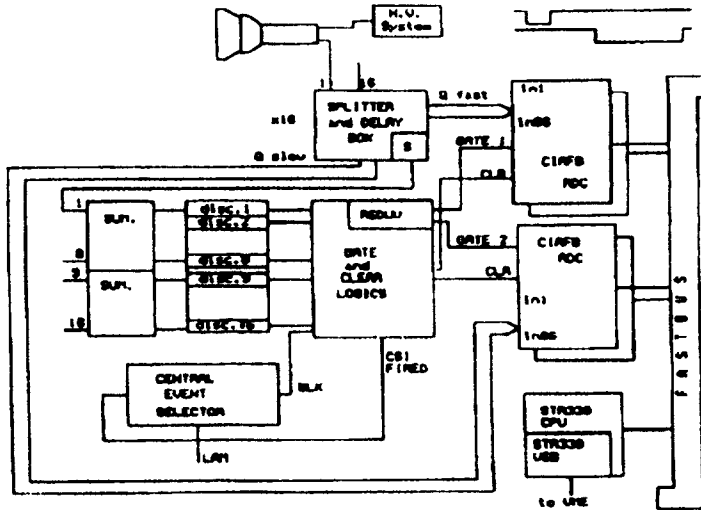


Fig. 16 The data acquisition system of the CsI(Tl) detectors.

In a FASTBUS Mini-Crate there are the STR 330 / CPU CERN Host Interface FASTBUS processor board, the STR330 / VSB I/O-Port and the STR 330 / LAN Ethernet module. The STR 330 is a 68030-based processor system. The STR 330 / VSB I/O-Port provides an efficient interface between the CHIPS and the ELTEC VME workstation. The STR 330 / VSB operates in VDB Slave mode. The CHIPS data memory is directly mapped into the local VSB address space and the VME EUROCOM-6 processor module is treated by the same manner as any local memory.

The ELTEC VME workstation is connected to a special Ethernet segment and further by a fiber-optic link to the μ VAX and SUN computers in the computer center (fig. 17).

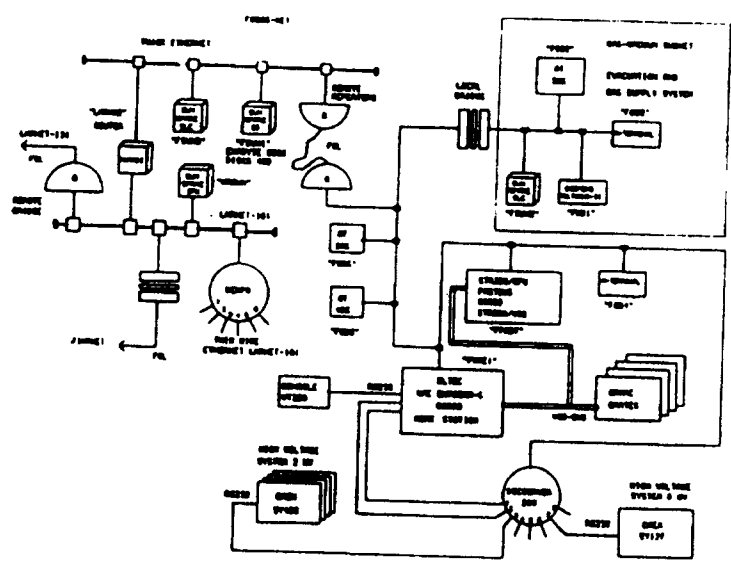


Fig. 17 Architecture of the FOBOS network.

The real-time operating system OS-9 (professional) released by Microware is used for the 68030 based VME and FASTBUS CHIPS modules. All time-critical tasks of the data acquisition are moved to the VME and FASTBUS processors.

The HOOPSY data acquisition software system resident at the μ VAX has been modified for VME EUROCOM-6 and successfully applied in the first FOBOS experiments. The data collected on the disk of the SUN Sparcstation-10 can be stored on Exabyte tape.

Quasi on-line monitoring of recorded data is performed by several PC's with the help of the ATHENE on-line/off-line data analysis program having access via LAN to the data just written on the SUN disk. The data file structure is characterized by sequential event storage into closed blocks of fixed length. All events are stored completely. The information about the data file structure is assigned to the program by header blocks.

8. DATA ANALYSIS SOFTWARE

An extensive software package has been developed for measurement data processing and analysis. Partly, available software has been adapted or modified.

The main tasks of these programs are an advanced on-line data monitoring, the multidimensional spectrum accumulation and event or parameter filtering, the calibration and correction of the raw data, the simulation of detector responses and acceptances as well as the physical off-line data analysis.

In a measurement with the complete FOBOS array more than 1000 parameters are defined to be partially recorded for the triggered events. Typically, the data base of an experiment amounts to about 10 Gbyte.

The ATHENE data analysis program originally developed for IBM AT PC's has been adapted to the NDP environment. It is arranged in the two global sections of data handling and spectrum representation and analysis. The input data format can be CAMDA, HOOPSY or OLYMP.

Most of the information is deduced from a two-dimensional data representation (matrix) with resolutions of some hundred channels per parameter. The color display allows to roughly visualize the content per channel (number of correlations). With the CPU Intel486-DX66 about 800 events per second can be accumulated into the permanent spectra memory of 50 matrixes with 350×350 channels. With the help of a menu or by use of the appropriate graphical tool (mouse control), the user can define the parameter limits and a number of selection criteria (up to 30 gates) interactively. All functions can be used as in the quasi on-line (fig. 18) as in the off-line mode.

A new program version ATHENE94 has been developed for SUN- and DEC stations what considerably increases the processing power and allows a batch-job mode. Modification can be easily done for any computer provided with an UNIX-like operational system and C++ and FORTRAN compilers as well as MOTIV/X11 and CERMLIB libraries. The input formats are HOOPSY and OLYMP. The latter is the standard output format. Accumulated histograms and colored scatterplots can be stored as PostScript or T_EX metafiles. The interactive dialog and the graphical data representation are accessible from a remote X - terminal. All user-defined initialization and selection specifications can be stored as ASCII-files and further

used to filter the event data into output-file. Fig. 19 gives an example of data representation by ATHENE94. The events selected by the gate in the Bragg-peak-height over energy matrix of a BIC (fig. 19a) are recorded into a histogram (fig. 19b) illustrating the charge resolution for IMF.

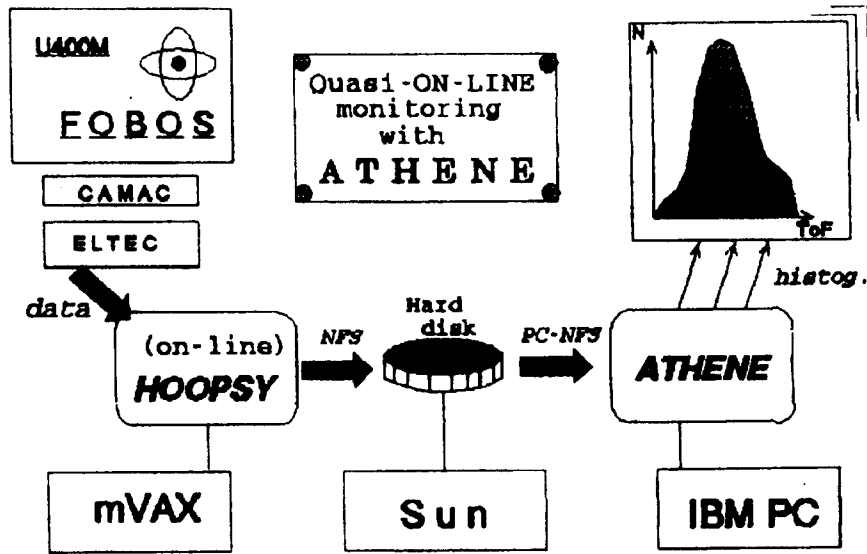


Fig. 18 The quasi on-line data monitoring with ATHENE.

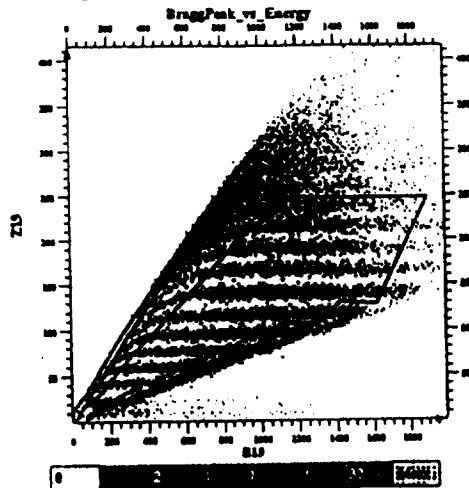


Fig. 19a Selection of events by setting a gate on the scatterplot.

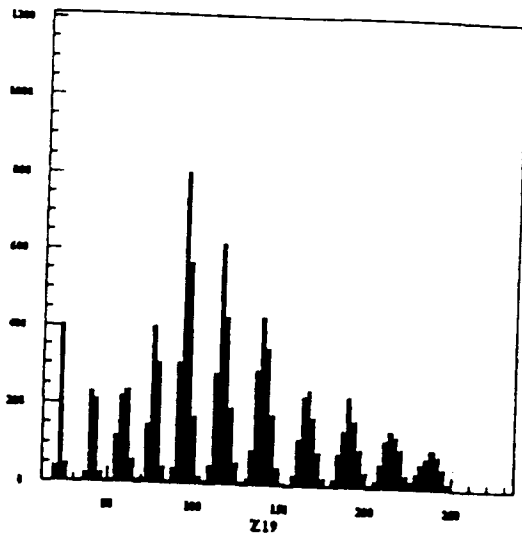


Fig. 19b Charge histogram of events filtered by the gate of fig. 19a.

Raw data filtering as well as further data analysis can also be carried out effectively by use of the OLYMP data processing package.

The program ORION has been developed for event simulation to evaluate the FOBOS acceptances.

The program HERAKLES applies an algorithm to identify the fragment mass from the measured velocity (TOF) and residual energy in the BIC. Namely heavy fragments (FF) can lose a considerable part of their energy ($> 50\%$) penetrating the PSAC and BIC window foils. Applying a certain iterative procedure to correct for this energy loss the original fragment mass distribution is reconstructed with an average uncertainty of about $3 + 4$ mass units in the unfavorable case of fission fragments from a $^{248}\text{Cm}(sf)$ source. For this purpose, an adjusted set of range-energy relations had to be created, and the nuclear stopping had to be taken into account. It is true, the charge-mass correlation must be known.

9. PILOT EXPERIMENTS WITH THE FOBOS DETECTORS

In the course of testing the FOBOS detectors and all the service systems a series of pilot experiments was carried out at the heavy-ion cyclotron U - 400 of the FLNR at incident beam energies slightly above the Coulomb-barrier energy. There, the two-detector- module test stand "Mini-FOBOS" has been used. The reactions chosen were ^{84}Kr (4.3 A MeV) + $^{116,118}\text{Sn}$ and ^{40}Ar (5.5 A MeV and 10 A MeV) + ^{194}Pt . The two gas-filled detectors were arranged at $\vartheta_1 = 45^\circ$, $\varphi_1 = 270^\circ$ and $\vartheta_2 = 45^\circ$, $\varphi_2 = 90^\circ$ in the first case and $\vartheta_1 = 105^\circ$, $\varphi_1 = 270^\circ$ and $\vartheta_2 = 45^\circ$, $\varphi_2 = 90^\circ$ in the

second case. Here in addition, a small parallel-plate avalanche counter (PPAC) was installed at $\theta_3 = 20^\circ$, $\varphi_3 = 270^\circ$ to detect projectile-like fragments (PLF). Besides small PPAC's were arranged near the target to perform an independent TOF measurement for both fragments registered.

Besides methodical investigations, reaction analysis has been carried out concerning the recoils from the elastic scattering of ^{84}Kr (ER) as well as the compound nucleus decay (RP). Applying the TKE-systematics of Viola, ER and RP could be selected. Total reaction cross-sections (σ_i) have been deduced from the RP/ER ratios which are in agreement with literature values. The σ_i for ^{116}Sn has been found to be higher by a factor of about 5 than for ^{118}Sn what could be related to the yield of an additional reaction component not present at ^{118}Sn . The result is illustrated in fig. 20.

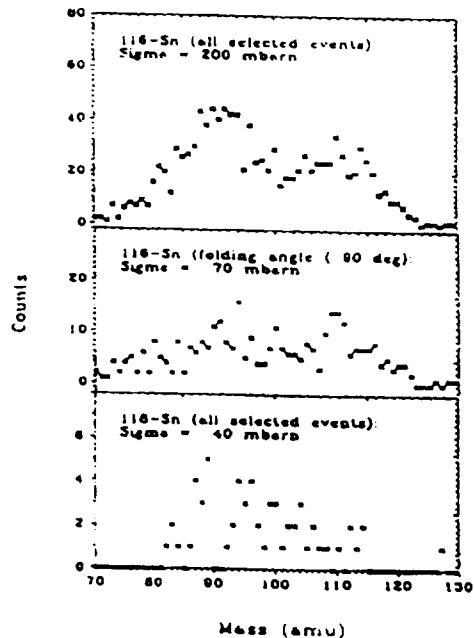


Fig. 20 Mass distributions of RP from $^{84}\text{Kr} + ^{116}\text{Sn}$.

A model-independent balance analysis has been performed for the fission products emitted after incomplete fusion of ^{40}Ar with ^{194}Pt applying the known folding-angle method to proof the usually considered massive-transfer model formalism. The correlation between the mass and the momentum transfer has been studied to estimate the number of neutrons evaporated. This is a measure for the excitation energy (E^*) deposited after incomplete fusion.

A qualitative picture is given in fig. 21. While fission at 5.5 A MeV beam energy occurs after complete fusion, at 10 A MeV two groups of fragments are observed corresponding to large and small transferred linear momenta (LMT), i.e., to nearly central and peripheral collisions, respectively. Indeed, at small LMT, several triple events could be registered where the PLF were hitting the third counter.

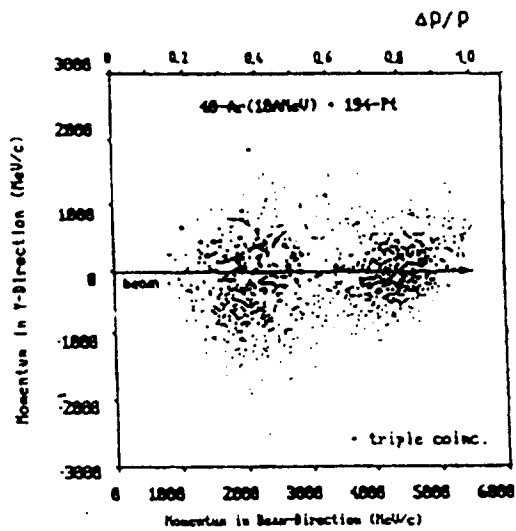


Fig. 21 Total fragment momentum distribution for ^{40}Ar (10 A MeV) + ^{194}Pt .

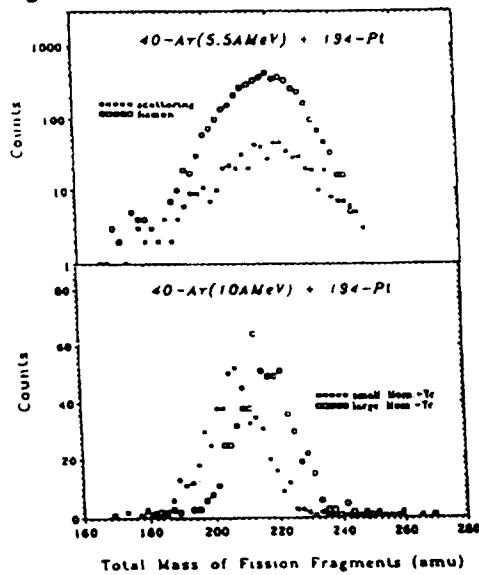


Fig. 22 Total fragment mass distributions for ^{40}Ar + ^{194}Pt at 5.5 and 10 A MeV.

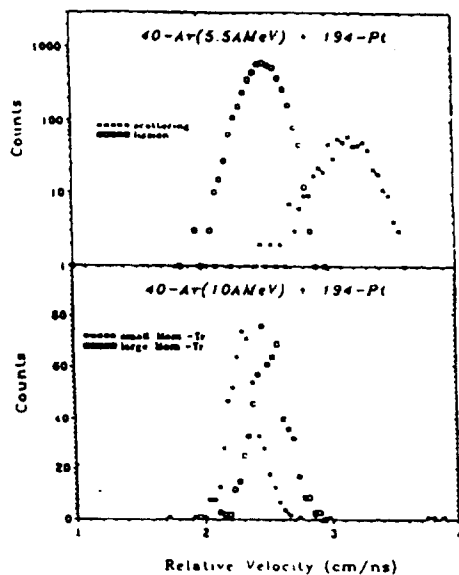


Fig. 23 Distributions of the relative velocity of fission fragments (corr. to fig. 21).

The total fragment mass distributions and the corresponding relative fragment velocities are given in fig. 22 and fig. 23. The deduced numbers of evaporated neutrons are smaller than the theoretical estimates for the assumed E^* , but their difference for the two groups of fragments is well reproduced. The main conclusion is that this method of evaluation of E^* after incomplete fusion is a valuable tool, mainly for events of a higher multiplicity, where the folding-angle method can not be applied.

10. SPONTANEOUS FISSION STUDIES

The apparatus parameters of FOBOS are well suited for the investigation of spontaneous fission. The long flight path is favorable for applying the TOF - TOF method. The PSAC well stand at the high counting rates obviously induced by the radioactive alpha decay. Start-detectors have to be used to perform the timing. Binary and ternary spontaneous fission has been investigated for $^{244}\text{Cm}(\text{sf})$ and $^{252}\text{Cf}(\text{sf})$.

The mass-energy distribution (M,TKE) of $^{244}\text{Cm}(\text{sf})$ has been studied including the regions of cold compact (CCF) and cold deformed (CDF) fission where the mass spectra are characterized by prominent structures caused by shell and pairing effects.

The resolving power of FOBOS is sufficient to identify the FF masses with $\Delta M \leq 3$ amu (fig. 24). About 10^5 FF coincidences have been recorded.

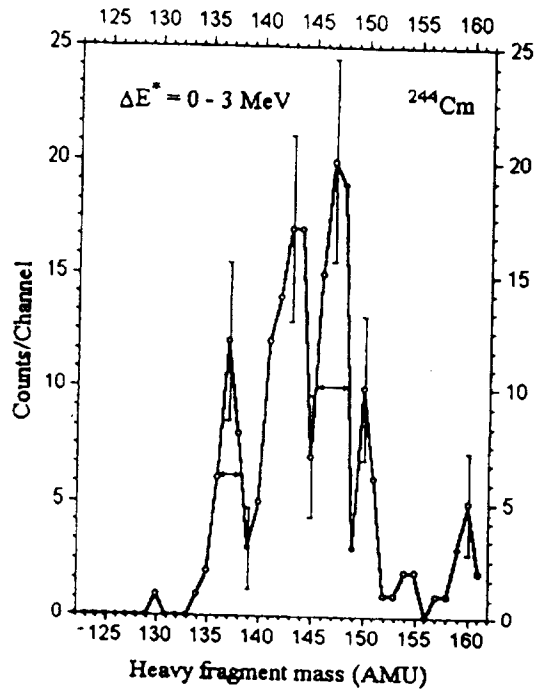


Fig. 24 FF mass distribution for CCF of $^{244}\text{Cm}(sf)$.

As an initial result of the measurement, the yield functions $Y(M,E)$ and $Y(M,TKE)$ were obtained. Here, M means the mass of the primary fragment and E - its kinetic energy. In order to analyze the fine-structure of the mass yield at different excitation energies (E^*) of the fissioning system at the scission point, the distribution $Y(M,TKE)$ has been transformed into a function $Y(M,E^*)$, where $E^* = Q - TKE$ and Q means the mean reaction energy for the production of fragments with a fixed mass ratio. The calculated $Q(M)$ are weighted mean values over available $Q_{Max}(M)$. We used a Gaussian weight-function with $FWHM = 3$ amu, corresponding to the mass resolution obtained.

Three cuts through the $Y(M,E^*)$ distribution are presented in fig. 25, namely, at low, medium and high E^* . One observe that in the CCF region the yields around the double-magic fragment $A_H = 132$ are highly suppressed. These masses, on the other hand, dominate in the yields at high E^* values. Fine structures smoothed at medium

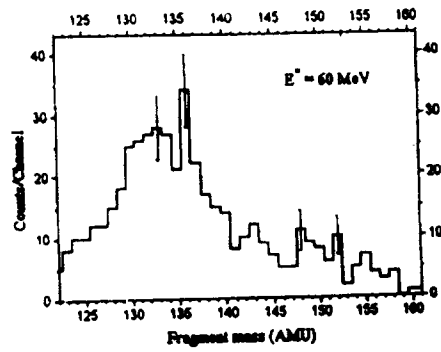
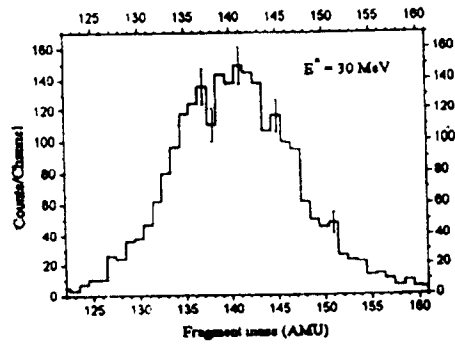
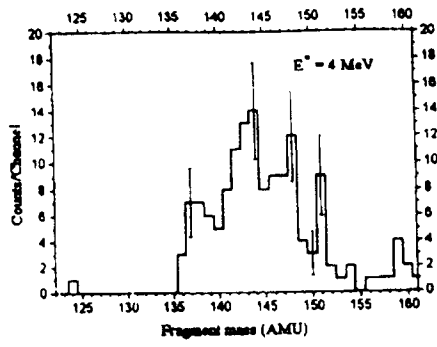


Fig. 25 Mass spectra of $^{244}\text{Cm}(sf)$ for three excitation energy windows of 1 MeV.

E^* appear again at diminishing TKE (increasing E^*). This is usually interpreted as the appearance of CDF.

The general tendency of the mass yield for the lighter fission fragment of $^{244}\text{Cm}(sf)$ in dependence on E^* can be seen from the contour plot of fig.26. There, the lines connect regions of equal conditional probability $P(M|E^*)$ for the formation of a fragment with the mass M at E^* . From this figure it is easy to get the function $E^*_{Y_{\max}} = \alpha \cdot (M - 96)$ for the dependence of the excitation energy at maximum yield on the mass of the lighter fragment. The result can be qualitatively interpreted in the frame of the cluster conception of multi-modal fission.

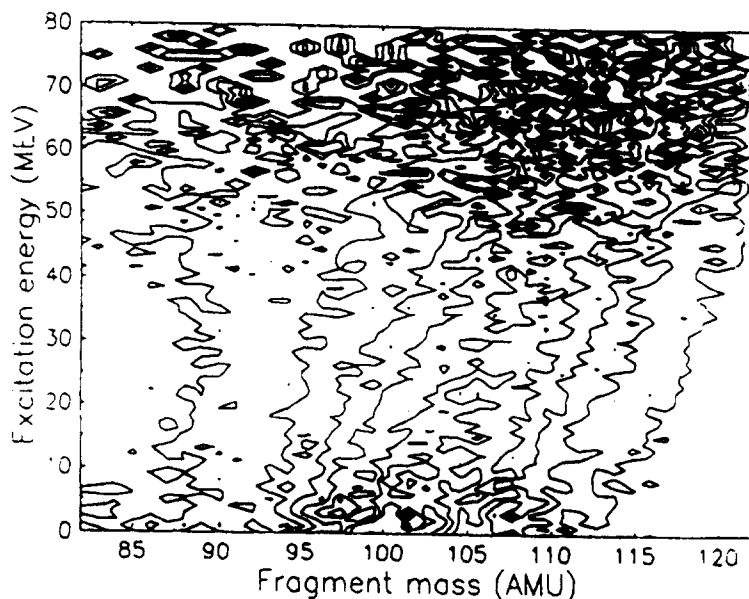


Fig. 26 Contour map of the conditional probability $P(M | E^*)$ for the formation of a fission fragment with mass M at E^* .

Ternary events, where an additional third particle is emitted, also were registered in this experiment. The main component of LCP and clusters in ternary spontaneous fission is due to long-range alpha particles (LRA) emitted from the neck region of the fissioning nucleus at the scission point. They are focused by the Coulomb field of the FF into directions nearly perpendicular to the fission axis.

Therefore, a CsI(Tl)-module of the scintillator shell was positioned at $\approx 90^\circ$ to the symmetry axis of the Start-detector aperture. Ternary alpha particles were well separated from the gamma rays applying pulse-shape discrimination.

As a result, a value of 3.24 ± 0.63 LCP per 10^3 sf has been obtained which is in agreement with the only other value available.

A high resolution measurement was carried out with $^{252}\text{Cf(sf)}$. About $5 \cdot 10^7$ fission fragment coincidences are recorded. The data analysis is yet in progress.

11. BEAM EXPERIMENTS

At present, several questions concerning the fission of hot nuclei (e.g. the influence of the dynamics on time scales, the mechanism of dissipation and others) are being extensively discussed. One goal of the experiments, being carried out presently at FOBOS, is the further investigation of IMF- and LCP-accompanied fission. Special interest is directed to the neck emission of IMF in fission of hot heavy nuclei, recently observed in the reaction $^3\text{He} (270 \text{ MeV}) + ^{232}\text{Th}$.

In the first beam experiment with FOBOS carried out in October 1993, a $270 \mu\text{g}/\text{cm}^2$ thick ^{232}Th target, deposited on a $50 \mu\text{g}/\text{cm}^2$ Al_2O_3 backing, was placed in the center of the FOBOS array and bombarded by a ^7Li beam from the U-400 M cyclotron. FF and IMF were registered by 10 PSAC measuring the TOF and the emission angle, and by 12 BIC measuring the energy and the Bragg-peak height. LCP were registered by 10 CsI(Tl) counters.

Since the U-400 M beam parameters did not allow a precise TOF measurement against the RF-signal of the cyclotron, two transmission PPAC had to be placed near the target for providing timing reference signals. They considerably limited the possible acceptance.

Altogether, $3 \cdot 10^6$ events with two FF have been recorded. They contain 230 triple (IMF-FF-FF) coincidences. The FF and IMF were selected by windows in the TOF-E and E-Z distributions.

As a first result of this experiment, yields of the IMF-accompanied fission related to the binary fission have been determined in dependence on E^* of the intermediate system and the angle between the fission axis and the direction of IMF emission ($\vartheta_{\text{IMF-FF}}$). The 230 triple events allow only a rough division into some intervals in E^* and $\vartheta_{\text{IMF-FF}}$.

The geometrical acceptance factors ε_{ijk} for all combinations with one FF in module i , a second FF in module j and an IMF in module k have been determined with the help of Monte-Carlo simulations. These simulations deliver mean excitation energies (E^*_{ijk}), which were assumed to be proportional to the LMT, as well as mean angles (ϑ_{ijk}).

With the numbers $N_{\text{IMF}(i,j,k)}$ of triple and $N_{\text{FF}(i,j)}$ of binary events for a certain combination of FOBOS modules (i,j,k) the measured IMF yield per fission (into the full solid angle 4π) becomes $Y_{i,j,k} = N_{\text{IMF}(i,j,k)} / (N_{\text{FF}(i,j)} \cdot \varepsilon_{ijk})$.

These yields have been sorted into groups of low LMT ($\Delta p \approx 50\%$; $E^* \approx 150$ MeV) and high LMT ($\Delta p \approx 80\%$; $E^* \approx 230$ MeV). The yields for five mean angles $\vartheta_{\text{IMF-FF}}$ are shown in fig. 27.

The $Y_{i,j,k}$ at low LMT do not show any significant variation for $\vartheta_{\text{IMF-FF}}$ between 35° and 90° . The mean value of this IMF- component amounts to $(0.67 \pm 0.08) \cdot 10^{-3}$ IMF-accompanied fissions per binary fission. At the higher LMT this value increases to $(2.31 \pm 0.28) \cdot 10^{-3}$

The enhanced yield near $\vartheta_{\text{IMF-FF}} \approx 90^\circ$ for higher E^* confirms the existence of a further IMF-source, the strength of which increases with E^* too. Possibly, these IMF were emitted from the neck region of the fissioning system at scission.

If one considers an interval $\Delta\vartheta_{\text{IMF-FF}} = 10^\circ$ around $\vartheta_{\text{IMF-FF}} = 90^\circ$, a rough estimation of the probability for neck emission of IMF results in a value of several units multiplied by 10^{-4} per binary fission. It is higher by about one order of magnitude than in the case of low energy (spontaneous or thermal neutron induced) ternary fission.

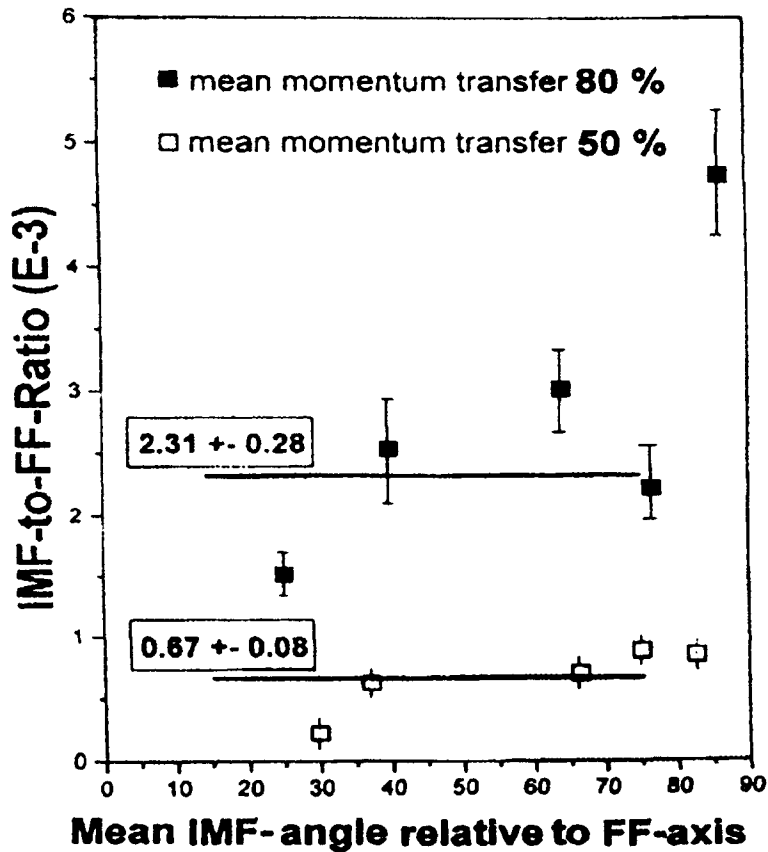


Fig.27 Yields $Y_{i,j,k}$ for certain mean IMF-angles ϑ_{ijk} according to low (open squares) and high (full squares) E^*_{ijk} .

These investigations were continued with the reaction ^{14}N (34 AMeV) + ^{197}Au in a more complete geometry of FOBOS. 16 gas-filled modules were used. 80 CsI(Tl) detectors of the FOBOS scintillator shell were operated in a slave-mode with respect to the gas detectors to register LCP and penetrating light fragments. One of the PPAC's was moved to a position at $\theta = 101^\circ$ to trigger on backward emitted fragments and, therefore, to lower the registration threshold in the forward positioned respective gas-detector for registration of very heavy fragments.

About $2.5 \cdot 10^6$ events with two and $2 \cdot 10^3$ events with three fragments hitting the gas modules have been recorded. A first estimate of the ratio of triple (FF+FF+IMF) to binary (FF+FF) decays yields $\approx 2.5 \cdot 10^{-3}$ for events with 80% LMT. This value is comparable with the value obtained for $^7\text{Li} + ^{232}\text{Th}$. The larger statistics in this experiment, however, allows a more detailed analysis.

The CsI(Tl) detectors recorded one additional LCP in $\approx 50\%$ of the events.

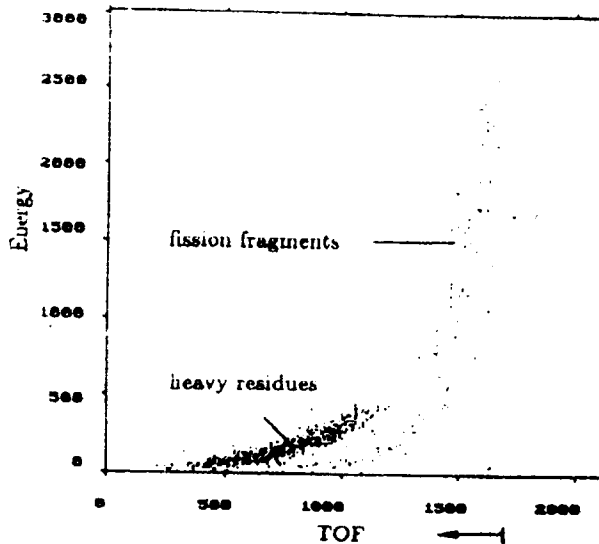


Fig. 28 Energy over TOF scatterplot of a gas-detector module at $\theta = 37.4^\circ$.

As it is shown in fig. 28, the chosen arrangement was able to register also heavy residues, being the heavier partners of a much lighter fragment emitted in a binary decay in backward direction.

Several conclusions can be drawn from a first data scan:

- (i) There is a smooth transition from a symmetric to a very asymmetric fission ($A_1/A_2 \approx 10$) both in the yield and in the fragment energy.
- (ii) In coincidence with a sideward emitted light fragment (IMF), either a heavy residue (ER) or fission fragments are emitted.
- (iii) Both in a symmetric and in an asymmetric fission there is a considerable probability of LCP emission in backward directions.

On completing this analysis now in progress, new information about the competition between binary and ternary decay of hot nuclei with mass $A \approx 190$ at excitation energy $E^* \approx 300$ MeV as well as about the probability for survival of a heavy residue is expected.

REFERENCES

H.-G. Ortlepp, H. Sodan, M. Andrassy, W.-D. Fromm, C.-M. Herbach, K.-H. Kaun, G. Pausch, W. Scidel, W. Wagner, H. Homeyer, H. Fuchs, T. Dietterle, G. Renz, M. Danziger, F. Gleisberg, W. Meiling, A.S. Fomichev, A.I. Ivanenko, I.V. Kolesov, Yu.E. Penionzhkevich, Yu.Ts. Oganessian, L.A. Rubinskaya, O.V. Strekalovsky, V.M. Vasko, A. Budzanowski

FOBOS - Ein 4π - Fragmentspektrometer (Zweite Ausbaustufe) Report ZfK - 734, Zentralinstitut für Kernforschung Rossendorf, Deutschland, November 1990.

Experimentvorschläge für das 4π - Fragmentspektrometer FOBOS
Berichte der Arbeitstagung der FOBOS - Kollaboration, Dresden, Deutschland, April 1991,

Report ZfK - 751, Zentralinstitut für Kernforschung Rossendorf (Ed. H. Sodan) Rossendorf, Dezember 1991 (Nachdruck Juni 1992).

H.-G. Ortlepp, M. Andrassy, G.G. Chubarian, M. Danziger, T. Dietterle, A.S. Fomichev, Sh.M. Heinitz, C.-M. Herbach, A.I. Ivanenko, I.V. Kolesov, D. May, Yu.Ts. Oganessian, Yu.E. Penionzhkevich, G. Renz, L.A. Rubinskaya, O.V. Strekalovsky, V.M. Vasko, W.-D. Fromm, K. Heidel, H. Sodan, W. Wagner, B.A. Burova, S.V. Radnev, I.D. Sandrev

The FOBOS 4π - Detector of Charged Particles at Dubna
Proc. of the Internat. Conf. on Exotic Nuclei, Foros, Crimea, Ukraine, October 1 - 5, 1991 (Ed. Yu.E. Penionzhkevich, R. Kalpakchieva) World Scientific, Singapore, 1991.

M. Andrassy, B.A. Burova, M. Danziger, T. Dietterle, A.S. Fomichev, W.-D. Fromm, K. Heidel, Sh.M. Heinitz, C.-M. Herbach, A.I. Ivanenko, I.V. Kolesov, H.-G. Ortlepp, Yu.Ts. Oganessian, Yu.E. Penionzhkevich, S.V. Radnev, G. Renz, L.A. Rubinskaya, I.D. Sandrev, H. Sodan, O.V. Strekalovsky, V.M. Vasko, W. Wagner

Present status of the FOBOS 4π - array (and further contributions)
Scientific Report 1989 - 1990, Laboratory of Nuclear Reactions, Joint Institute for Nuclear Research, Dubna, Russia, JINR E7 - 91 - 75 (Ed. B.I. Pustylnik) Dubna, 1991, p.171.

- H.-G. Ortlepp, H. Sodan, M. Andrassy, W.-D. Fromm, C.-M. Herbach, K.-H. Kaun, G. Pausch, W. Scidel, W. Wagner, H. Homeyer, H. Fuchs, T. Dietterle, G. Renz, M. Danziger, F. Gleisberg, W. Meiling, A.S. Fomichev, A.I. Ivanenko, I.V. Kolesov, Yu.E. Penionzhkevich, Yu.Ts. Oganessian, L.A. Rubinskaya, O.V. Strelakovsky, V.M. Vasko, A. Budzanowski
- The 4π - Fragment spectrometer FOBOS
Frühjahrstagung DPG e.V., Darmstadt, Deutschland, 1991, Verhandl. der DPG.
- G. Pausch, H. Fuchs, H. Homeyer, G. Röschert, C. Schwarz, A. Siwek, W. Terlau, A. Tutay, B. Bochev, W. Wagner, A. Matthies, W. Kantor
- Production of intermediate mass fragments in $960 \text{ MeV } ^{32}\text{S} + \text{Au}$
Annual Report 1991, HMI - 497, Hahn - Meitner - Institut GmbH, Berlin, Deutschland, 1992, p.83.
- H.-G. Ortlepp, M. Andrassy, G.G. Chubarian, M. Danziger, T. Dietterle, A.S. Fomichev, Sh.M. Heinitz, C.-M. Herbach, A.I. Ivanenko, I.V. Kolesov, D. May, Yu.Ts. Oganessian, Yu.E. Penionzhkevich, G. Renz, L.A. Rubinskaya, O.V. Strelakovsky, V.M. Vasko, W.-D. Fromm, K. Heide, H. Sodan, W. Wagner, B.A. Burova, S.V. Radnev, I.D. Sandrev
- The FOBOS 4π - detector of charged particles at Dubna
Proc. of the Int. Conf. on New Nuclear Physics with Advanced Techniques, Ierapetra, Crcte. Grece, June 23 - 29, 1991 (Ed. F.A. Beck, S. Kossionides & C.A. Kalfas) World Scientific, Singapore, 1992, p.302.
- H. Fuchs, H. Homeyer, G. Pausch, W. Terlau, C. Schwarz, A. Siwek, B. Bochev, W. Wagner, A. Budzanowski, W. Kantor
- Multiple break - up of nuclei : Experiments with ARGUS
at the Hahn - Meitner - Institut Berlin
Proc. of the 10th Internat. School on Nuclear Physics, Neutron Physics and Nuclear Energy, Varna, Bulgaria, October 14 - 19, 1991.
- FOBOS - a 4π - Fragment spectrometer for heavy - ion reaction products
Report FZR 92 - 11, Forschungszentrum Rossendorf e.V., Germany
(Ed. H.-G. Ortlepp, K.-D. Schilling) 1992.

A.S. Fomichev, H.-G. Ortlepp, Yu.E. Penionzhkevich, C.-M. Herbach,
I. David, W. Wagner, G. Pausch, H. Sodan, V.A. Vitenko
Basic characteristics of the scintillation phoswich detectors of the
4 π - set - up FOBOS
Preprint P15 - 92 - 50, Joint Institute for Nuclear Research, Dubna,
Russia, 1992 (in Russian).

H. Fuchs, H. Homeyer, G. Pausch, G. Röscher, C. Schwarz, A. Sourell,
W. Terlau, A. Tutay, A. Budzanowski, W. Kantor, A. Siwek, W. Wagner
Study of intermediate - mass fragment emission and multifragmentation
with 30 AMeV ^{32}S projectiles
Frühjahrstagung DPG e.V., Salzburg, Österreich, 24 - 28. 2 1992.
Verhandl. der DPG.

H.-G. Ortlepp, M. Andrassy, G.G. Chubarian, M. Danziger, A.S. Fomichev,
C.-M. Herbach, A.I. Ivanenko, I.V. Kolesov, Yu.Ts. Oganessian,
Yu.E. Penionzhkevich, G. Renz, O.V. Strelakovsky, V.M. Vasko, A. Matthies,
W. Wagner, H. Fuchs, D. Hilscher, H. Homeyer, W. von Oertzen, G. Pausch
The 4 π - Fragment spectrometer FOBOS
Book of Abstracts of the Internat. Nucl. Physics Conf., Wiesbaden, Germany,
July 26 - August 1, 1992, Nr. 5.2.

H.-G. Ortlepp, M. Andrassy, G.G. Chubarian, M. Danziger, L. Dietterle,
A.S. Fomichev, P. Gippner, C.-M. Herbach, I.A. Ivanenko, I.V. Kolesov,
A. Matthies, D. May, Yu.Ts. Oganessian, Yu.E. Penionzhkevich, V.N. Pokrovsky,
G. Renz, L.A. Rubinskaya, O.V. Strelakovsky, V.V. Trofimov, V.M. Vasko,
K. Heide, K.-D. Schilling, W. Seidel, H. Sodan, W. Wagner, H. Fuchs,
D. Hilscher, W. von Oertzen, G. Pausch, P. Ziem, V.E. Zhuchko
Status of the 4 π - Fragment spectrometer FOBOS

- a) Annual Report 1992, Institute of Nuclear and Hadronic Physics,
Forschungszentrum Rossendorf e.V., Germany, FZR - 93 - 10
(Ed. F. Döna, H. Prade) Rossendorf, 1993, pp.93-100 and pp.122-137.
- b) Scientific Report 1991 - 1992, Flerov Laboratory of Nuclear Reactions,
Joint Institute for Nuclear Research, Dubna, Russia, JINR E7 - 93 - 57
(Ed. B.I. Pustynnik) Dubna, 1993, pp.240-253.

G. Pausch, J. Krüger, W. Seidel, W. Wagner, C.-M. Herbach, A. Matthies,
H.-G. Ortlepp, V.V. Trofimov, V.E. Zhuchko, H. Fuchs, H. Homeyer,
G. Röscher, A. Tutay, P. Ziem, A. Budzanowski, A. Siwek, L. Zrodowski
Extension of the ARGUS phoswich - array by a FOBOS gas - detector module and
test of the FOBOS data acquisition system

Annual Report 1992. HMI - 507. Hahn - Meitner - Institut GmbH, Berlin, Deutschland. 1993. p.87

M. Andrassy, G.G. Chubarian, A.S. Fomichev, P. Gippner, Sh. Heinitz, C.-M. Herbach, A. Matthies, H.-G. Ortlepp, G. Renz, O.V. Strekalovsky, G. Pausch, K.-D. Schilling, W. Wagner
Heavy - ion reaction experiments at the Dubna U - 400M cyclotron using detectors of the FOBOS array
ibid., p.75.

M. Andrassy, G.G. Chubarian, M. Danziger, P. Gippner, L. Dietterle, A.S. Fomichev, H. Fuchs, K. Heidel, C.-M. Herbach, D. Hilscher, H. Homeyer, I.A. Ivanenko, I.V. Kolesov, A. Matthies, D. May, Yu.Ts. Oganessian, W. von Oertzen, H.-G. Ortlepp, G. Pausch, Yu.E. Penionzhkevich, G. Renz, K.-D. Schilling, H. Sodan, O.V. Strekalovsky, V.V. Trofimov, V.M. Vasko, W. Wagner, P. Ziem
FOBOS - ein 4π - Detektor mit niedriger Energieschwelle für Schwerionenreaktionsprodukte
Frühjahrstagung DPG e.V., Mainz, Deutschland, 22 - 26. 3. 1993, Verhandl. DPG (VI) 28 (1993) S.565.

M. Andrassy, G.G. Chubarian, P. Gippner, C.-M. Herbach, A. Matthies, H.-G. Ortlepp, G. Pausch, G. Renz, K.-D. Schilling, W. Wagner
Analyse der Massen- und Impulsbilanz bei Messungen von Fragmenten aus Schwerionenreaktionen
Frühjahrstagung DPG e.V., Mainz, Deutschland, 22. - 26. 3. 1993, Verhandl. DPG (VI) 28 (1993) S.634.

W. Wagner, A.S. Fomichev, H.-G. Ortlepp, C.-M. Herbach, A. Matthies, G. Pausch, O.V. Strekalovsky, M.A. Milovidov, V.A. Vitenko
A large area CsI(Tl) detector for the scintillator shell of FOBOS
JINR Rapid Communications 4 [61] - 93, Joint Institute for Nuclear Research, Dubna, Russia. 1993. p.49.

H.-G. Ortlepp, M. Andrassy, G.G. Chubarian, M. Danziger, P. Gippner, L. Dietterle, A.S. Fomichev, C.-M. Herbach, A.I. Ivanenko, I.V. Kolesov, A. Matthies, D. May, Yu.Ts. Oganessian, Yu.E. Penionzhkevich, V.N. Pokrovsky, G. Renz, L.A. Rubinskaya, O.V. Strekalovsky, V.V. Trofimov, V.M. Vasko, K. Heidel, K.-D. Schilling, W. Seidel, H. Sodan, W. Wagner, V.E. Zhuchko, H. Fuchs, D. Hilscher, H. Homeyer, P. Ziem, G. Pausch, B.A. Burova, S.V. Radnev, I.D. Sandrev

The 4 π - Fragment spectrometer FOBOS - Status and first preliminary results -
Proc. of the Internat. School-Seminar on Heavy Ion Physics, Dubna, Russia,
May 10 - 15, 1993, JINR E7 - 93 - 274, vol. 2
(Ed. Yu.Ts. Oganessian, Yu.E. Penionzhkevich, R. Kalpakchieva)
Dubna, 1993, p.466.

A.A. Aleksandrov, I.A. Aleksandrova, M. Andrassy, L. Dietterle, V.N. Doronin,
P. Gippner, C.-M. Herbach, D. Hilscher, S.A. Ivanovsky, J. Krüger, A. Matthies,
D. May, H.-G. Ortlepp, G. Pausch, Yu.E. Penionzhkevich, V.N. Pokrovsky,
G. Renz, K.D. Schilling, D.I. Shishkin, O.V. Strekalovsky, V.V. Trofimov,
C. Umlauf, D.V. Vakarov, V.M. Vasko, W. Wagner, V.E. Zhuchko
Fission and IMF emission in the reaction 43 AMeV ^7Li on ^{232}Th studied with
FOBOS
Annual Report 1993, Institute of Nuclear and Hadronic Physics, Forschungszentrum
Rossendorf e.V., Germany, FZR - 35 (Ed. F. Dönau, H. Prade) Rossendorf, 1994,
pp.55-61 and pp.90-113.

J. Krüger, A. Budzanowski, H. Fuchs, C.-M. Herbach, H. Homeyer,
D.V. Kamanin, A. Matthies, H.-G. Ortlepp, G. Pausch, G. Röscher,
W. Seidel, A. Siwek, V.V. Trofimov, A. Tutay, W. Wagner, R. Wolski,
P. Ziem, V.E. Zhuchko
Investigation of IMF emission and projectile fragmentation in the system
 ^{32}S (960 MeV) + ^{197}Au with the extended ARGUS detector
ibid., p.61.

M. Andrassy, L. Dietterle, V.N. Doronin, P. Gippner, K. Heide, C.-M. Herbach,
D. Hilscher, S.A. Ivanovsky, J. Krüger, A. Matthies, D. May, H.-G. Ortlepp,
G. Pausch, Yu.E. Penionzhkevich, G. Renz, K.-D. Schilling, D.I. Shishkin,
O.V. Strekalovsky, V.V. Trofimov, C. Umlauf, D.V. Vakarov, V.M. Vasko,
W. Wagner, Th. Wilpert, V.E. Zhuchko
Analyse von leichten, intermediären und Spaltfragmenten in der Reaktion
 ^7Li (43 AMeV) + ^{232}Th mit dem Multidetektorsystem FOBOS
Frühjahrstagung DPG e.V., München, Deutschland, 21. - 25. 3. 1994,
Verhandl. DPG (VI) 29 (1994) S.1888.

J. Krüger, A. Budzanowski, H. Fuchs, C.-M. Herbach, D. Hilscher, H. Homeyer,
D. Kamanin, A. Matthies, H.-G. Ortlepp, G. Pausch, W. Seidel, A. Siwek,
V.V. Trofimov, A. Tutay, W. Wagner, R. Wolski, L. Zrodowski, V.E. Zhuchko
Untersuchung der Projekttilfragmentation und IMF - Emission im System
 ^{32}S (960 MeV) + ^{197}Au am erweiterten ARGUS - Detektor

Frühjahrstagung DPG e.V. München, Deutschland. 21. - 25. 3. 1994,
Verhandl. DPG (VI) 29 (1994) S 1945.

A.S. Fomichev, I. David, S.M. Lukyanov, Yu.E. Penionzhkevich, N.K. Skobelev,
O.B. Tarasov, A. Matthies, H.-G. Ortlepp, W. Wagner, M. Lewitowicz,
M.G. Saint-Laurent, J.M. Corre, Z. Dlouhy, I. Pecina, C. Borcea
The response of a large CsI(Tl) detector to light particles and heavy ions in the
intermediate energy range

Preprint JINR P13 - 93 - 114, Joint Institute for Nuclear Research, Dubna,
Russia, 1993

Report GANIL P 93 23, Laboratoire Commun IN2P3 (CNRS) - D.S.M (CEA),
Caen, France, 1993.

Nucl. Instr. and Meth. in Phys. Research A 344, 1994, p 378.

A. Siwek, A. Sourell, A. Budzanowski, H. Fuchs, H. Homeyer, G. Pausch,
W. Kantor, G. Röscher, C. Schwarz, W. Terlau, A. Tutay

Multifragmentation study on 30 A MeV $^{32}\text{S} + ^{58}\text{Ni}$

Preprint HMI / FK - Fuc1 Hahn - Meitner - Institut GmbH, Berlin, Deutschland,
1994.

H.-G. Ortlepp, M. Andrassy, G.G. Chubarian, M. Danziger, T. Dietterle,

A.S. Fomichev, Sh.M. Heinitz, C.-M. Herbach, A.I. Ivanenko, I.V. Kolesov,

D. May, Yu.Ts. Oganessian, Yu.E. Penionzhkevich, G. Renz, L.A. Rubinskaya,

O.V. Strelakovsky, V.M. Vasko, W.-D. Fromm, K. Heide, H. Sodan, W. Wagner,

B.A. Burova, S.V. Radnev, I.D. Sandrev

The FOBOS 4 π - detector of charged particles at Dubna

Proc. of the Internat. Workshop on Physical Experiments and First Results on the
Heavy Ion Storage and Cooler Rings, Smolenice, Slovakia, June 1 - 5, 1992,

JINR E 7 - 94 - 270, Dubna, Russia, 1994, p.388.

Yu.V. Pyatkov, A.A. Aleksandrov, I.A. Aleksandrova, B.I. Andreev, P. Gippner,

C.-M. Herbach, E.M. Kozulin, Matthies, Yu.Ts. Oganessian, H.-G. Ortlepp,

Yu.E. Penionzhkevich, G. Renz, K.-D. Schilling, O.V. Strelakovsky, V.M. Vasko,

W. Wagner

Two-velocities measurements of fragment spectra in ^{244}Cm cold spontaneous
fission on the FOBOS spectrometer

Internat. Workshop on Nuclear Fission and Fission Product Spectroscopy, Château
de la Baume, Seyssins, France, May 2 - 4, 1994 (Ed. H. Faust & G. Fioni)

Grenoble, 1994, p.144

A.A. Aleksandrov, I.A. Aleksandrova, M. Andrassy, L. Dietterle, V.N. Doronin, P. Gippner, C.-M. Herbach, D. Hilscher, S.A. Ivanovsky, A. Matthies, D. May, H.-G. Ortlepp, G. Pausch, Yu.E. Penionzhkevich, V.N. Pokrovsky, G. Renz, K.-D. Schilling, D.I. Shishkin, O.V. Strelalovsky, V.V. Trofimov, C. Umlauf, D.V. Vakarov, V.M. Vasko, W. Wagner, V.E. Zhuchko

First experiments with FOBOS

Proc. of the 5th Internat. Conf. on Nucleus-Nucleus Collisions, Taormina, Italy, May 30 - June 4, 1994 (Ed. M. Di Toro, E. Migneco and P. Piattelli) North-Holland, Amsterdam, 1995, Nucl. Phys. A583 (1994) 465c

O.V. Strelalovsky, K. Heidei, S.A. Ivanovsky, D. May, H.-G. Ortlepp, G. Pausch, G. Renz, V.V. Trofimov, I.P. Tsurin, W. Wagner, V.E. Zhuchko
The front - end electronics and the data acquisition system of the FOBOS 4π - array

Proc. of the 16th Internat. Symp. on Nuclear Electronics, Varna Bulgaria, September 12 - 18, 1994. (to be published)

O.V. Strelalovsky, H.-G. Ortlepp, V.V. Trofimov, V.E. Zhuchko
The data acquisition system of the FOBOS 4π - array
Proc. of the Internat. ESONE Conf. on Real - Time Data Systems, Dubna, Russia, August 1994. (to be published)

Yu.V. Pyatkov, A.A. Aleksandrov, I.A. Aleksandrova, B.I. Andreev, P. Gippner, C.-M. Herbach, E.M. Kozulin, A. Matthies, Yu.Ts. Oganessian, H.-G. Ortlepp, Yu.E. Penionzhkevich, G. Renz, K.-D. Schilling, O.V. Strelalovsky, V.M. Vasko, W. Wagner

Cold spontaneous fission of ^{244}Cm studied at FOBOS

a) Scientific Report 1993 - 1994, Flerov Laboratory of Nuclear Reactions, Joint Institute for Nuclear Research, Dubna, Russia.
(to be published at JINR Dubna)

b) Annual Report 1994, Institute of Nuclear and Hadronic Physics, Forschungszentrum Rossendorf e.V., Germany. (to be published)

A.A. Aleksandrov, I.A. Aleksandrova, M. Andrassy, L. Dietterle, V.N. Doronin, P. Gippner, C.-M. Herbach, D. Hilscher, S.A. Ivanovsky, A. Matthies, D. May, H.-G. Ortlepp, G. Pausch, Yu.E. Penionzhkevich, V.N. Pokrovsky, G. Renz, K.-D. Schilling, D.I. Shishkin, O.V. Strelalovsky, V.V. Trofimov, C. Umlauf, D.V. Vakarov, V.M. Vasko, W. Wagner, V.E. Zhuchko
Correlations between intermediate mass and fission fragments in the reaction ^7Li (43 AMeV) on ^{232}Th studied at FOBOS

- a) Scientific Report 1993 - 1994. Flerov Laboratory of Nuclear Reactions, Joint Institute for Nuclear Research, Dubna, Russia. (to be published at JINR Dubna)
- b) Annual Report 1994. Institute of Nuclear and Hadronic Physics, Forschungszentrum Rossendorf e.V., Germany. (to be published)

A.A. Aleksandrov, I.A. Aleksandrova, L. Dietterle, V.N. Doronin, S. Dshemuchadse, P. Gippner, C.-M. Herbach, S.A. Ivanovsky, D.V. Kamanin, A. Matthies, D. May, H.-G. Ortlepp, G. Pausch, Yu.E. Penionzhkevich, G. Renz, K.D. Schilling, D.I. Shishkin, O.V. Strelakovsky, V.V. Trofimov, I.P. Tsurin, C. Umlauf, D.V. Vakarov, V.M. Vasko, W. Wagner, V.E. Zhuchko
 Study of fission and IMF emission in the reaction ^{14}N (34 A MeV) on ^{197}Au at FOBOS

- a) Scientific Report 1993 - 1994. Flerov Laboratory of Nuclear Reactions, Joint Institute for Nuclear Research, Dubna, Russia. (to be published at JINR Dubna)
- b) Annual Report 1994. Institute of Nuclear and Hadronic Physics, Forschungszentrum Rossendorf e.V., Germany. (to be published)

H.-G. Ortlepp, W. Wagner, A.A. Aleksandrov, I.A. Aleksandrova, L. Dietterle, V.N. Doronin, P. Gippner, C.-M. Herbach, D. Hilscher, S.A. Ivanovsky, A. Matthies, Yu.Ts. Oganessian, G. Pausch, Yu.E. Penionzhkevich, G. Renz, K.-D. Schilling, D.I. Shishkin, O.V. Strelakovsky, V.V. Trofimov, C. Umlauf, D.V. Vakarov, V.M. Vasko, V.E. Zhuchko, A.G. Artukh, G.F. Gridnev, M. Grushezki, J. Szmidler, Yu.G. Teterev, M.G. Nagaenko, Yu.M. Sereda, I.N. Vishnevski, S.G. Genchev
 The COMBAS - fragment - separator of radioactive nuclei and the FOBOS - 4π - detector for charged particles
 Proc. of the Internat. Workshop on Physics with Recoil Separators and Detector Arrays, New Delhi, India, January 30 - February 2, 1995 (Allied Publishers Ltd.) New Delhi, 1995. (submitted to the publisher)

H.-G. Ortlepp, C.-M. Herbach, W. Wagner, P. Gippner, A. Matthies, G. Pausch, Yu.E. Penionzhkevich, G. Renz, K.-D. Schilling, O.V. Strelakovsky, V.E. Zhuchko
 Fission and emission of intermediate - mass fragments in asymmetric heavy - ion collisions
 Internat. Nuclear Physics Conference, Beijing, China, August 21 - 26, 1995. (submitted abstract)

Status reports, contributions and experiment proposals for FOBOS
Proceedings of the FOBOS workshop '94, Cracow, Poland, June 28 - 30, 1994
(Ed. W. Wagner) FZR - 65, Rossendorf, Germany, 1995.

H.-G. Ortlepp, A.A. Aleksandrov, I.A. Aleksandrova, L. Dietterle, V.N. Doronin,
P. Gippner, C.-M. Herbach, S.A. Ivanovsky, D.V. Kamanin, A. Matthies,
G. Pausch, Yu.E. Penionzhkevich, G. Renz, K.-D. Schilling, D.I. Shishkin,
O.V. Strelakovsky, V.V. Trofimov, I.P. Tsurin, C. Umlauf, D.V. Vakarov,
V.M. Vasko, W. Wagner, V.E. Zhuchko

Spectroscopy of correlated fragments from the fission of hot nuclei performed
at the FOBOS 4π - array

Internat. Conf. on Low Energy Nuclear Dynamics (LEND '95),
St. Petersburg, Russia, 1995. (submitted abstract)

Yu.V. Pyatkov, A.A. Aleksandrov, B.I. Andreev, P. Gippner, C.-M. Herbach,
Yu.Ts. Oganessian, H.-G. Ortlepp, Yu.E. Penionzhkevich, R.A. Shekhmamet'ev,
W. Wagner

Structure peculiarities in the mass - energy spectrum of the $^{244}\text{Cm(sf)}$ fission
fragments studied at the FOBOS set-up
ibid. (submitted abstract)

Received by Publishing Department
on March 30, 1995.

Принимается подписка на препринты, сообщения Объединенного института ядерных исследований и «Краткие сообщения ОИЯИ».

Установлена следующая стоимость подписки на 12 месяцев на издания ОИЯИ, включая пересылку, по отдельным тематическим категориям:

Индекс	Тематика	Цена подписки на год
1.	Экспериментальная физика высоких энергий	22600 р.
2.	Теоретическая физика высоких энергий	59200 р.
3.	Экспериментальная нейтронная физика	7800 р.
4.	Теоретическая физика низких энергий	23400 р.
5.	Математика	14800 р.
6.	Ядерная спектроскопия и радиохимия	12000 р.
7.	Физика тяжелых ионов	2200 р.
8.	Криогеника	1400 р.
9.	Ускорители	12200 р.
10.	Автоматизация обработки экспериментальных данных	12200 р.
11.	Вычислительная математика и техника	14300 р.
12.	Химия	1200 р.
13.	Техника физического эксперимента	21300 р.
14.	Исследования твердых тел и жидкостей ядерными методами	7200 р.
15.	Экспериментальная физика ядерных реакций при низких энергиях	2600 р.
16.	Дозиметрия и физика защиты	2200 р.
17.	Теория конденсированного состояния	12200 р.
18.	Использование результатов и методов фундаментальных физических исследований в смежных областях науки и техники	1800 р.
19.	Биофизика	1800 р.
	«Краткие сообщения ОИЯИ» (5—6 выпусков)	15000 р.

Подписка может быть оформлена с любого месяца года.

Организациям и лицам, заинтересованным в получении изданий ОИЯИ, следует перевести (или отправить по почте) необходимую сумму на расчетный счет 000608905 Дубненского филиала ММКБ, г.Дубна Московской области, п/инд. 141980 МФО 211844, указав: «За подписку на издания ОИЯИ».

Во избежание недоразумений необходимо уведомить издательский отдел о произведенной оплате и вернуть «Карточку подписчика», отметив в ней номера и названия тематических категорий, на которые оформляется подписка, по адресу:

141980 г. Дубна Московской обл.
ул.Жолио Кюри, 6
ОИЯИ, издательский отдел

**SUBJECT CATEGORIES
OF THE JINR PUBLICATIONS**

Index	Subject
1.	High energy experimental physics
2.	High energy theoretical physics
3.	Low energy experimental physics
4.	Low energy theoretical physics
5.	Mathematics
6.	Nuclear spectroscopy and radiochemistry
7.	Heavy ion physics
8.	Cryogenics
9.	Accelerators
10.	Automatization of data processing
11.	Computing mathematics and technique
12.	Chemistry
13.	Experimental techniques and methods
14.	Solid state physics. Liquids
15.	Experimental physics of nuclear reactions at low energies
16.	Health physics. Shieldings
17.	Theory of condensed matter
18.	Applied researches
19.	Biophysics

Андраши М. и др.

E7-95-148

ФОБОС 4 π -детектор заряженных частиц
в Лаборатории ядерных реакций им.Г.Н.Флерова
Объединенного института ядерных исследований, Дубна

Представлены параметры 4 π -спектрометра ФОБОС, а также первые результаты физических исследований на нем.

Работа выполнена в Лаборатории ядерных реакций им.Г.Н.Флерова
ОИЯИ.

Сообщение Объединенного института ядерных исследований. Дубна, 1995

Andrassy M. et al.

E7-95-148

The FOBOS 4 π -Detector of Charged Particles at the FLNR
of the JINR Dubna

The parameters of the FOBOS 4 π -spectrometer and first results of physical investigations performed at this facility are presented.

The investigation has been performed at the Flerov Laboratory of Nuclear Reactions, JINR.

Communication of the Joint Institute for Nuclear Research. Dubna, 1995

Макет Т.Е.Попеко

Подписано в печать 5.04.95
Формат 60×90/16. Офсетная печать. Уч.-изд.листов 3,01
Тираж 400. Заказ 48114. Цена 1806 р.

Издательский отдел Объединенного института ядерных исследований
Дубна Московской области